



HAL
open science

Security Control of Autonomous Ground Vehicles Under DoS Attacks via a Novel Controller with the Switching Mechanism

Yunshuai Ren, Xiangpeng Xie, Anh-Tu Nguyen

► **To cite this version:**

Yunshuai Ren, Xiangpeng Xie, Anh-Tu Nguyen. Security Control of Autonomous Ground Vehicles Under DoS Attacks via a Novel Controller with the Switching Mechanism. IEEE Transactions on Fuzzy Systems, inPress, 10.1109/TFUZZ.2024.3381264 . hal-04522881

HAL Id: hal-04522881

<https://hal.science/hal-04522881>

Submitted on 27 Mar 2024

HAL is a multi-disciplinary open access archive for the deposit and dissemination of scientific research documents, whether they are published or not. The documents may come from teaching and research institutions in France or abroad, or from public or private research centers.

L'archive ouverte pluridisciplinaire **HAL**, est destinée au dépôt et à la diffusion de documents scientifiques de niveau recherche, publiés ou non, émanant des établissements d'enseignement et de recherche français ou étrangers, des laboratoires publics ou privés.

Security Control of Autonomous Ground Vehicles Under DoS Attacks via a Novel Controller with the Switching Mechanism

Yunshuai Ren, Xiangpeng Xie, *Senior Member, IEEE*, and Anh-Tu Nguyen, *Senior Member, IEEE*

Abstract—This paper focuses on the security tracking control problem of nonlinear autonomous ground vehicles (AGVs) under Denial-of-Service (DoS) attacks. In order to resist DoS attacks and other external disturbances, a new security control scheme is proposed. Firstly, the Takagi-Sugeno (T-S) fuzzy system is established to represent the nonlinear AGV system under DoS attacks. In particular, in order to improve the flexibility of control and reduce the impact of DoS attacks on tracking control, a novel controller with a specific switching mechanism is designed. The switching mechanism relies on fuzzy membership functions, which can make better use of nonlinear vehicle speed information. Secondly, the sufficient conditions to ensure global exponential stability of the T-S fuzzy-based switched system are given by using the Lyapunov function method. Finally, the simulation platform built by Carsim and Matlab/Simulink is used to verify the effectiveness of the proposed control scheme.

Index Terms—Cyber-physical systems, DoS attacks, security control, autonomous ground vehicles, Takagi-Sugeno fuzzy system, switching mechanism.

I. INTRODUCTION

VEHICLES are an important means of transportation at present, which can provide great convenience for people's travel. But at the same time, due to the improper operation of human beings, it also brings serious traffic problems. As an important vehicle assistance technology, automatic driving plays a key role in improving driving safety, liberating human drivers, and improving driving comfort [1]. Based on this, perfect AGVs are expected to solve current traffic problems and improve driving safety. Recently, many research results have emerged to achieve this goal [2], [3]. The emergence of these achievements continues to promote the development of autonomous vehicles. But until now, a completely automatic vehicle driving control method still has many challenges, such as control accuracy, driving comfort, driving safety, and so on. These challenges still take a lot of time and effort to overcome. This also motivates our research interest in autonomous vehicles.

This work was supported in part by the National Natural Science Foundation of China under Grant 62373196. (*Corresponding author: Xiangpeng Xie.*)

Yunshuai Ren is with the College of Electrical Engineering, Sichuan University, Chengdu 610065, China (e-mail: 17863656118@163.com).

Xiangpeng Xie is with the School of Internet of Things, Nanjing University of Posts and Telecommunications, Nanjing 210023, China (e-mail: xiexiangpeng1953@163.com).

Anh-Tu Nguyen is with LAMIH laboratory, UMR CNRS 8201, Université Polytechnique Hauts-de-France, 59313 Valenciennes, France, and also with INSA Hauts-de-France, 59313 Valenciennes, France (e-mail: t-nguyen@uphf.fr).

Vehicle tracking control is the premise of realizing automatic driving. The final effect of tracking control is to achieve tracking without error, or the tracking error meets the specific requirements of people. With the further research of tracking control, many research results have been obtained, such as PID control [4], [5], sliding mode control (SMC) [6]–[8], H_∞ control [9]–[11], model predictive control (MPC) [12]–[14], adaptive control [15], [16], etc. PID method has the characteristic of simple structure and does not need to consider vehicle information. Such as, only cross-tracking error information was considered in [5], and a PID controller was designed for the trajectory maneuver of the autonomous vehicle. Meanwhile, the disadvantage brought by the simple structure is that the resources of the vehicle are not utilized enough. In contrast, SMC, MPC, and H_∞ control can make better use of the dynamic information of the vehicle itself and provide more theoretical possibilities. Such as, in [7], the virtual desired input was considered, and an SMC method was given to realize the path tracking of AGVs. The time-varying velocity and other vehicle information were considered in [10] to design controllers for AGVs with four-wheel steering. In [13], the vehicle information such as thrust limitation and safe operating area in the autonomous underwater vehicle (AUV) system was considered, and an MPC method was studied for the AUV. After studying the above literature, it is found that the rich dynamic information such as time-varying velocity and nonlinear tire force of vehicles can be used to carry out vehicle modeling and tracking control. Therefore, how to make better use of these dynamic information and improve the tracking effect of the algorithm on the basis of the existing is the focus of our next research.

With the improvement of computer computing power, artificial intelligence continues to develop. Network communication as an important part of improving vehicle intelligence, its security has been widely concerned. The security of communication mainly faces the challenge of various cyber attacks [17]–[19]. These malicious attacks on tracking control are highly likely to cause serious traffic accidents. To this end, it is necessary to study the security control strategy for AGVs. In general, the following two types of network attacks are mainly considered: false data injection (FDI) [20], [21] and DoS attacks [22]–[24]. DoS attacks are a kind of network attack that interrupts communication. When the attack occurs, the data packet information needed at the time cannot be obtained. DoS attacks have the characteristics of simple attack methods and low attack cost, and have gradually become a

common means of network attacks. When the DoS attacks occur, the system will be equivalent to an open-loop control state. If not dealt with in time, it is likely to cause the vehicle to lose control, resulting in serious consequences. At present, in order to deal with DoS attacks, researchers have given many security control strategies [25]–[29]. For example, in [26], the security of a networked suspension system under periodic DoS attacks was studied. A new H_∞ control method via event-triggered mechanism (ETM) was designed. Compared with periodic DoS attacks, non-periodic DoS attacks are more universal. In [27], a security control method was given for the 5-degree-of-freedom active semi-vehicle suspension system to deal with the non-periodic DoS attacks. The characteristics of DoS active and dormant was fully considered and an improved ETM was established. With the deepening of the research on DoS attacks, in order to be more suitable for practical application, the research gradually develops from single DoS attacks to hybrid network attacks. The object of its practical application is becoming more and more rich. The lateral control problem of networked unmanned vehicle systems was studied in [28]. An asynchronous elastic ETM was given to solve the interference of hybrid network attacks on vehicle tracking control. In [29], for the unmanned surface vehicles (USVs) system, a collaborative design scheme was given to study the control problem of the USVs system when it encounters communication delay, communication failure, and DoS attacks interference. Through the study of the above literature, it is found that the intelligence of vehicles is accompanied by the security problem of network communication. The purpose of the research on DoS attacks and other network attacks is to better fit the practical application. At present, although DoS attacks have achieved certain results in suspension systems and vehicle systems, there is still room for improvement in the theoretical research of AGV tracking control under DoS attacks, which also stimulates our research interest in improving vehicle tracking control accuracy and driving safety.

Based on the above motivation, a new security control scheme is proposed to effectively ensure the performance of AGVs under DoS attacks. The main contributions are as follows:

- 1) A novel fuzzy controller with a switching mechanism is designed that can select the appropriate fuzzy controller according to the speed information of the vehicle tracking process. Compared with the traditional form of controller [30], it makes better use of the dynamic information of the vehicle and effectively enhances the tracking capability of AGVs in different road scenarios.
- 2) An enhanced security control scheme is proposed for AGVs to deal with non-periodic DoS attacks. The sufficient conditions are derived by the fuzzy-based switched system and the novel fuzzy controller, which ensure exponential stability and weighted H_∞ performance of nonlinear AGVs.

Notation: $(H)^* \triangleq H + H^T$, H denotes the square matrix. ‘*’ denotes a block of matrices that can be derived by symmetry. ‘ $H < 0$ ’ indicates the matrix H is negative definite, and ‘ $H > 0$ ’ indicates the matrix H is positive definite.

TABLE I
PARAMETERS OF VEHICLE

Symbols	Description	Unit
C_f/C_r	Front/Rear cornering stiffness	N/rad
l_f/l_r	Distance from front/rear axle to CG	m
F_{xf}/F_{xr}	Front/Rear longitudinal forces	N
α_f/α_r	Front/Rear sideslip angle	deg
v_x/v_y	Longitudinal/Lateral speed	km/h
M	Vehicle mass	kg
I_z	Inertia's moment around z-axis	kg m ²
x_p	Distance of look-ahead	m
δ	The steering angle of the front wheel	deg
ρ	Road curvature	1/m
r	Yaw rate	deg/s
$e_p/\Delta\psi$	Lateral/Heading error	m
β	Vehicle body sideslip angle	deg

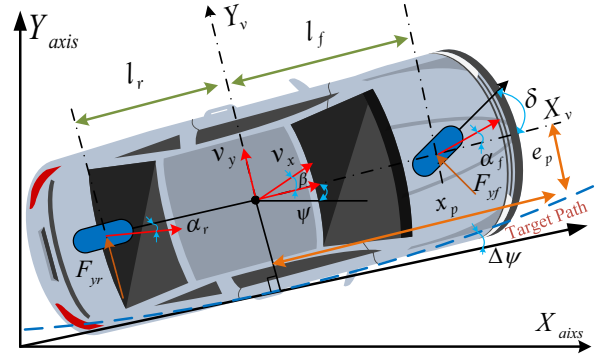


Fig. 1. Dynamic models of vehicle and road.

II. VEHICLE SYSTEM MODELLING

This section mainly completes two tasks: One is to introduce the modeling process of the vehicle and road dynamics models. Second, a T-S fuzzy modeling technique for nonlinear vehicle models is presented, which can reduce design conservatism.

A. Nonlinear Vehicle Dynamics Model

In this paper, the vehicle is assumed to use front-wheel steering, and the single-track model shown in Fig. 1 is adopted for path tracking. This model contains the basic dynamic information related to path tracking, which is convenient for the design of subsequent schemes. The related symbols in Fig. 1 are given in Table I. The nonlinear vehicle dynamics model is considered as [31]:

$$\begin{aligned} M(\dot{v}_x - rv_y) &= F_{xf} \cos \delta - F_{yf} \sin \delta + F_{xr} \\ M(\dot{v}_y + rv_x) &= F_{xf} \sin \delta + F_{yf} \cos \delta + F_{yr} \\ I_z \dot{r} &= l_f (F_{xf} \sin \delta + F_{yf} \cos \delta) - l_r F_{yr} \end{aligned} \quad (1)$$

Here, using small angle assumptions similar to those in [32]. Then, it can be obtained angle $\beta = \arctan\left(\frac{v_y}{v_x}\right) \approx \frac{v_y}{v_x}$. And, the angle α_f and α_r can be calculated by

$$\alpha_f = \delta - \frac{v_y + l_f r}{v_x}, \alpha_r = \frac{l_r r - v_y}{v_x} \quad (2)$$

Next, the forces F_{yf} and F_{yr} can be obtained by

$$F_{yf} = C_f \left(\delta - \frac{v_y + l_f r}{v_x} \right), F_{yr} = C_r \left(\frac{l_r r - v_y}{v_x} \right) \quad (3)$$

By combining the (1), (2) and (3), the vehicle lateral dynamics model can be obtained as

$$\begin{bmatrix} \dot{\beta} \\ \dot{r} \end{bmatrix} = \begin{bmatrix} a_{11} & a_{12} \\ a_{21} & a_{22} \end{bmatrix} \begin{bmatrix} \beta \\ r \end{bmatrix} + \begin{bmatrix} b_{11} \\ b_{21} \end{bmatrix} \delta \quad (4)$$

where

$$a_{11} = -\frac{(C_r + C_f)}{Mv_x}, a_{12} = \frac{(l_r C_r - l_f C_f)}{Mv_x^2} - 1, b_{11} = \frac{C_f}{Mv_x},$$

$$a_{21} = \frac{(C_r l_r - C_f l_f)}{I_z}, a_{22} = -\frac{(l_r^2 C_r + l_f^2 C_f)}{I_z v_x}, b_{21} = \frac{l_f C_f}{I_z}.$$

B. Vehicle-Road Dynamics Model

In order to achieve the purpose of automatic driving, obtain good path-tracking performance. On the basis of the above vehicle dynamics model, it is necessary to further establish the connection between the target path and the vehicle. This connection has been established in Fig. 1. Then, the above connection can be described by the following error model [33]:

$$\dot{e}_p = v_x \beta + v_x \Delta \psi + x_p r, \quad \Delta \psi = r - v_x \rho \quad (5)$$

Combining the vehicle lateral dynamics model (4) and error model (5), the dynamic model of vehicle and road is given as

$$\dot{x}(t) = Ax(t) + Bu(t) + E\omega(t) \quad (6)$$

where $x(t) = [\beta \quad r \quad e_p \quad \Delta \psi]^T$, $u(t) = \delta$, $\omega(t) = \rho$ and

$$A = \begin{bmatrix} a_{11} & a_{12} & 0 & 0 \\ a_{21} & a_{22} & 0 & 0 \\ v_x & x_p & 0 & v_x \\ 0 & 1 & 0 & 0 \end{bmatrix}, B = \begin{bmatrix} b_{11} \\ b_{21} \\ 0 \\ 0 \end{bmatrix}, E = \begin{bmatrix} 0 \\ 0 \\ 0 \\ -v_x \end{bmatrix}$$

In the process of automatic driving, the path error e_p is as small as possible to ensure the tracking accuracy, and the smooth change of steering input δ is conducive to ensuring the driving comfort. Based on the above two considerations and the ideas in [30], [34], a cost function is given as follows:

$$J = \int_0^\infty (\ell_1 e_q^2 + \ell_2 \Delta \psi^2 + \Re u^2) dt$$

$$= \int_0^\infty [(\nabla^{1/2} \bar{F} x)^T (\nabla^{1/2} \bar{F} x) + (\Re^{1/2} \bar{G} u)^T (\Re^{1/2} \bar{G} u)] dt \quad (7)$$

where $\ell_g > 0$, $g \in \{1, 2\}$, and $\Re > 0$ are the weighting coefficients and

$$\bar{F} = \begin{bmatrix} 0 & 0 & 1 & 0 \\ 0 & 0 & 0 & 1 \\ 0 & 0 & 0 & 0 \end{bmatrix}, \bar{G} = \begin{bmatrix} 0 \\ 0 \\ 1 \end{bmatrix}, \nabla = \begin{bmatrix} \ell_1 & 0 & 0 \\ 0 & \ell_2 & 0 \\ 0 & 0 & 0 \end{bmatrix}$$

Based on the above, the following expression for the controlled output is given:

$$z(t) = Fx(t) + Gu(t) \quad (8)$$

where $F = \nabla^{1/2} \bar{F}$, $G = \Re^{1/2} \bar{G}$. It can be easily obtained that $J = \int_0^\infty z^T(t) z(t) dt$. Here, based on the cost function (7), the controlled output (8) with weight coefficients is established. The introduction of weight coefficients ℓ_g and \Re brings more theoretical possibilities. By adjusting the values of the ℓ_g , and \Re weight coefficients, it is possible to achieve a more delicate control effect.

C. Vehicle-Road Model Based on T-S Fuzzy System

In the actual vehicle-driving process, the speed usually changes. Therefore, it is meaningful to consider the time-varying speed v_x in the process of modeling. Here, assume that the speed v_x is time-varying, where $v_x \in [v_{x \min}, v_{x \max}]$. Therefore, the above system (6) has parameters v_x , $\frac{1}{v_x}$ and $\frac{1}{v_x^2}$, where $v_x \in [v_{x \min}, v_{x \max}]$. If the sector nonlinearity approach [35] is used, these three parameters are treated as independent. It will increase the complexity and conservatism of the model. Therefore, to avoid this difficulty, consider the following variable substitution [36]:

$$\frac{1}{v_x} = \frac{1}{v_0} + \frac{1}{v_1} \varepsilon \quad (9)$$

where $v_0 = \frac{2v_{x \min} v_{x \max}}{v_{x \min} + v_{x \max}}$ and $v_1 = \frac{-2v_{x \min} v_{x \max}}{v_{x \max} - v_{x \min}}$. If $\varepsilon = \varepsilon_{\min} = -1$, it follows $v_x = v_{x \min}$. If $\varepsilon = \varepsilon_{\max} = 1$, then $v_x = v_{x \max}$. Based on the above substitution and Taylars approximation, one can get that $v_x \approx v_0 \left(1 - \frac{v_0}{v_1} \varepsilon\right)$ and $\frac{1}{v_x^2} \approx \frac{1}{v_0^2} \left(1 + 2\frac{v_0}{v_1} \varepsilon\right)$. Then, the vehicle-road model based on T-S fuzzy system can be presented as

$$\begin{cases} \dot{x}(t) = \sum_{i=1}^2 \eta_i(\varepsilon) (A_i x(t) + B_i u(t) + E_i \omega(t)) \\ z(t) = Fx(t) + Gu(t) \end{cases} \quad (10)$$

where $\eta_1 = \frac{|\varepsilon_{\max} - \varepsilon|}{\varepsilon_{\max} - \varepsilon_{\min}}$, $\eta_2 = \frac{|\varepsilon_{\min} - \varepsilon|}{\varepsilon_{\max} - \varepsilon_{\min}}$, $\Omega_1 = \Omega(\varepsilon_{\min})$, $\Omega_2 = \Omega(\varepsilon_{\max})$, $\Omega \in [A, B, E]$.

III. SECURITY CONTROL SCHEME BASED ON THE NOVEL CONTROLLER WITH SWITCHING MECHANISM

In this section, we will use the general T-S fuzzy system to develop the control scheme. The control scheme obtained by using the generalized T-S fuzzy system can be applied not only to the above vehicle system, but also to other real systems that can be modeled as T-S fuzzy systems. Based on the general T-S fuzzy system, we give a novel controller design idea with a switching mechanism. Meanwhile, considering the security communication problem of the vehicle system, the corresponding security control scheme is given in the scenario with or without DoS attacks.

A. System Description

For generality, the following T-S fuzzy system is considered:

$$\begin{cases} \dot{x}(t) = \sum_{i=1}^p \eta_i(\varepsilon) (A_i x(t) + B_i u(t) + E_i \omega(t)) \\ z(t) = \sum_{i=1}^p \eta_i(\varepsilon) (F_i x(t) + G_i u(t)) \end{cases} \quad (11)$$

where $x(t) \in \mathbb{R}^{n_x}$ denotes the system state vector, $u(t) \in \mathbb{R}^{n_u}$ denotes the control input, $\omega(t) \in \mathbb{R}^{n_\omega}$ denotes the disturbance, $z(t) \in \mathbb{R}^{n_z}$ denotes the controlled output. $\varepsilon \in [\varepsilon_1, \varepsilon_2, \dots, \varepsilon_p]^T$ denotes the premise variables. $\eta_i(\varepsilon)$ denotes the membership functions (MFs), where $\sum_{i=1}^p \eta_i(\varepsilon) = 1$ and $0 \leq \eta_i(\varepsilon) \leq 1$.

B. DoS Attacks

The cyber-attacks on the network channel of the AGV system are depicted in Fig. 2. It is assumed that the DoS occurs on the channel from controller to actuator. The n th DoS occurrence time-interval is defined as follows:

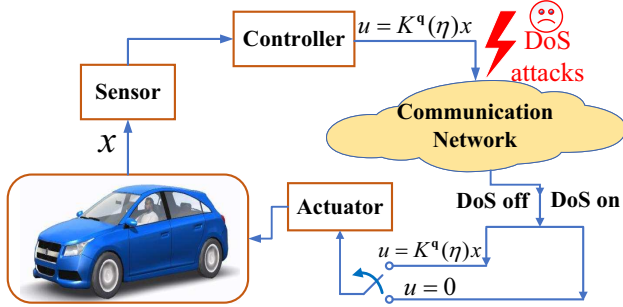


Fig. 2. Structure of the AGVs system under the DoS attacks.

$$H_n = [h_n, h_n + \tau_n), n \in \mathbb{N} \quad (12)$$

where $\{h_n\}_{n \in \mathbb{N}}$ denotes the status of the n th DoS from “off” to “on”, and τ_n denotes the duration of the n th DoS. Then, $t \in [0, +\infty)$, the allowed communication time-interval $\Theta(0, t)$ and the denied communication time-interval $\Xi(0, t)$ are expressed as $\Xi(0, t) = \bigcup_{n \in \mathbb{N}} H_n \cap [0, t]$, $\Theta(0, t) = [0, t] \setminus \Xi(0, t)$.

C. A Novel Controller with Switching Mechanism

To facilitate the design and application of the control scheme, the processing method similar to that in [36] is adopted, so that the controller and the above system (11) have the same MFs. The following novel controller with a switching mechanism is designed:

$$u(t, \mathbf{q}) = \sum_{i=1}^p \eta_i(\varepsilon) K_i^{\mathbf{q}} x(t) \quad (13)$$

where $K_i^{\mathbf{q}}$ denotes the controller gain. $\mathbf{q} \in \{1, \dots, p\}$ is obtained based on the following switching rules:

$$\eta_{\mathbf{q}}(\varepsilon) = \max\{\eta_i(\varepsilon), i \in \{1, \dots, p\}\} \quad (14)$$

Compared to traditional controller (15), at every moment of the vehicle’s operation, using the controller (13), there will be p group of fuzzy controllers available for scheduling. In contrast, the traditional controller (15) has only one set of controllers for the entire run time. Therefore, it can be considered that the novel controller has more theoretical possibilities in vehicle tracking control.

$$u(t) = \sum_{i=1}^p \eta_i(\varepsilon) K_i x(t) \quad (15)$$

REMARK 1. Note that time-varying speed v_x is an important dynamic information of vehicle. Making full use of this information is conducive to improving the effect of control. Therefore, it is meaningful to design the switching control mechanism based on the fuzzy MFs generated by speed v_x . In addition, MFs are a kind of weight coefficient, so it is

reasonable to choose the controller with the largest weight to execute first. Thirdly, the switching mechanism is designed in this way, without introducing other variables, which reduces the difficulty of implementation of the proposed controller in practical applications.

REMARK 2. The novel controller (13) needs to judge the switching mode at each moment during implementation because of the consideration of switching. This adds some of the burden of online computing. However, considering that the switching modes are limited, the traditional controller (13) also needs to calculate the fuzzy MFs, as well as the continuous improvement of the current computing power. The increased online computing burden will not have much impact on the application of the controller (13).

REMARK 3. Note that under the current switching rules (14), the number of switching modes is equal to the number of fuzzy rules. This is a limitation to further improve the control effect of the controller (13). To break this limitation, the existing switching mechanism needs to be upgraded. In the future, we consider adding a weighting factor μ to the existing switching rules (14). When $\eta_{\mathbf{q}} \geq \mu \sum_{j \in \{1, 2, \dots, p\}, j \neq \mathbf{q}} \eta_j$, p switching modes are designed. When $\eta_{\mathbf{q}} < \mu \sum_{j \in \{1, 2, \dots, p\}, j \neq \mathbf{q}} \eta_j$, another p switching modes are designed. Under the above switching rules, the flexibility of the controller will be effectively improved. This will bring more theoretical possibilities for enhancing tracking performance.

D. Controlled System with the Novel Controller

Consider a case where there are no DoS attacks, combining fuzzy system (11) and controller (13), it is obtained that

$$\begin{cases} \dot{x}(t) = \sum_{i=1}^p \sum_{j=1}^p \eta_i \eta_j [(A_i + B_i K_j^{\mathbf{q}}) x(t) + E_i \omega(t)] \\ z(t) = \sum_{i=1}^p \sum_{j=1}^p \eta_i \eta_j [F_i + G_i K_j^{\mathbf{q}}] x(t) \end{cases} \quad (16)$$

Consider another case where there are DoS attacks. The switched controller is designed as follows:

$$u(t) = \begin{cases} \sum_{i=1}^p \eta_i(\varepsilon) K_i^{\mathbf{q}} x(t), & t \in [h_{n-1} + \tau_{n-1}, h_n) \\ 0, & t \in [h_n, h_n + \tau_n) \end{cases} \quad (17)$$

Combining fuzzy system (11) and controller (17) yields the fuzzy-based switched system shown below:

$$\begin{cases} \dot{x}(t) = \begin{cases} \sum_{i=1}^p \sum_{j=1}^p \eta_i \eta_j [(A_i + B_i K_j^{\mathbf{q}}) x(t) + E_i \omega(t)], & t \in L_n \\ \sum_{i=1}^p \eta_i [A_i x(t) + E_i \omega(t)], & t \in H_n \end{cases} \\ z(t) = \begin{cases} \sum_{i=1}^p \sum_{j=1}^p \eta_i \eta_j [F_i + G_i K_j^{\mathbf{q}}] x(t), & t \in L_n \\ \sum_{i=1}^p \eta_i F_i x(t), & t \in H_n \end{cases} \end{cases} \quad (18)$$

where $L_n = [h_{n-1} + \tau_{n-1}, h_n)$.

DEFINITION 1. [37] Give scalars $\gamma > 0$ and $\alpha > 0$, if under zero initial conditions, $\omega(s) \in L_2[0, +\infty)$. The system is said to have a weighted H_∞ index (α, γ) , if it satisfies

$$\int_0^\infty e^{-\alpha s} z(s)^T z(s) ds \leq \gamma^2 \int_0^\infty \omega^T(s) \omega(s) ds \quad (19)$$

Assumption 1. [38] There exist $\epsilon \in [0, +\infty)$ and $\tau_D \in (0, +\infty)$ such that $n(\hat{\tau}, t) \leq \epsilon + \frac{t-\hat{\tau}}{\tau_D}$, where $n(\hat{\tau}, t)$, $t \geq \hat{\tau}$, represents the number of DoS conversion from "off" to "on".

Assumption 2. [38] There exist $\kappa \in [0, +\infty)$ and $T \in [1, +\infty)$ such that $|\Xi(\hat{\tau}, t)| \leq \kappa + \frac{t-\hat{\tau}}{T}$, where $|\Xi(\hat{\tau}, t)|$, $t \geq \hat{\tau}$, represents the length of $\Xi(\hat{\tau}, t)$.

REMARK 4. Note that since the attacker's energy is limited, and some system protection measures, such as gaussian filtering, spread spectrum technique, also constrain DoS attacks. Therefore, it is reasonable to assume that DoS attacks are limited in duration and frequency. If the duration and frequency of DoS attacks are not limited, it may cause the AGV system to open the loop. Therefore, the Assumption 1 and Assumption 2 need to be made.

In the actual process of vehicle automatic driving, the transient performance of the vehicle system is conducive to improving driving comfort. The concept of \mathcal{D} -stability can adjust the transient response of the system by limiting all eigenvalues of the system matrix \mathbf{A} to the LMI region $\mathcal{D}(\mathbf{a}, \mathbf{r})$. The following lemma is given to guarantee the \mathcal{D} -stability of matrix \mathbf{A} [39].

LEMMA 1. [39], [40] For matrix \mathbf{A} , given scalars \mathbf{a} , and \mathbf{r} , the matrix \mathbf{A} is \mathcal{D} -stable, if there exists a matrix $X > 0$, such that

$$\begin{bmatrix} -\mathbf{r}X & \mathbf{a}X + \mathbf{A}X \\ * & -\mathbf{r}X \end{bmatrix} \leq 0 \quad (20)$$

E. LMI-Based Security Control Design Without DoS Attacks

The following theorem gives sufficient conditions to ensure the stabilization of the system using a novel fuzzy controller with a switching mechanism in the absence of DoS attacks.

THEOREM 1. For given scalars $\gamma > 0$, $\ell_g > 0$, $\Re > 0$, \mathbf{a} , and \mathbf{r} , the system (16) is \mathcal{D} -stable with the H_∞ level, if there exists matrices $X > 0$, $Y_j^{\mathbf{q}}$, $Q_\zeta^{\mathbf{q}} > 0$, $U_\zeta^{\mathbf{q}} > 0$, with j , \mathbf{q} , $\zeta \in \{1, \dots, p\}$, such that

$$\Psi_{ii}^{\mathbf{q}} + \Pi_i^{\mathbf{q}} < 0, \text{ for } i \in \{1, 2, \dots, p\} \quad (21)$$

$$\Psi_{ij}^{\mathbf{q}} + \Psi_{ji}^{\mathbf{q}} + \hat{\Pi}_{ij}^{\mathbf{q}} < 0, \text{ for } 1 \leq i < j \leq p \quad (22)$$

$$\Upsilon_{ii}^{\mathbf{q}} + S_i^{\mathbf{q}} < 0, \text{ for } i \in \{1, 2, \dots, p\} \quad (23)$$

$$\Upsilon_{ij}^{\mathbf{q}} + \Upsilon_{ji}^{\mathbf{q}} + \hat{S}_{ij}^{\mathbf{q}} < 0, \text{ for } 1 \leq i < j \leq p \quad (24)$$

where

$$\Psi_{ij}^{\mathbf{q}} = \begin{bmatrix} \psi_{11} & E_i & \psi_{13} \\ * & -\gamma^2 I & 0 \\ * & * & -I \end{bmatrix}, \Upsilon_{ij}^{\mathbf{q}} = \begin{bmatrix} -\mathbf{r}X & \varphi_{12} \\ * & -\mathbf{r}X \end{bmatrix}$$

$$\Pi_i^{\mathbf{q}} = \begin{cases} \sum_{\zeta \in \{1, \dots, p\}, \zeta \neq \mathbf{q}} Q_\zeta^{\mathbf{q}}, & \text{for } i = \mathbf{q} \\ -Q_i^{\mathbf{q}}, & \text{for } i \neq \mathbf{q} \end{cases}$$

$$\hat{\Pi}_{ij}^{\mathbf{q}} = \begin{cases} \sum_{\zeta \in \{1, \dots, p\}, \zeta \neq \mathbf{q}} Q_\zeta^{\mathbf{q}} - Q_j^{\mathbf{q}}, & \text{for } i = \mathbf{q}, j \neq \mathbf{q} \\ \sum_{\zeta \in \{1, \dots, p\}, \zeta \neq \mathbf{q}} Q_\zeta^{\mathbf{q}} - Q_i^{\mathbf{q}}, & \text{for } i \neq \mathbf{q}, j = \mathbf{q} \\ -(Q_i^{\mathbf{q}} + Q_j^{\mathbf{q}}), & \text{for } i \neq \mathbf{q}, j \neq \mathbf{q} \end{cases}$$

$$S_i^{\mathbf{q}} = \begin{cases} \sum_{\zeta \in \{1, \dots, p\}, \zeta \neq \mathbf{q}} U_\zeta^{\mathbf{q}}, & \text{for } i = \mathbf{q} \\ -U_i^{\mathbf{q}}, & \text{for } i \neq \mathbf{q} \end{cases}$$

$$\hat{S}_{ij}^{\mathbf{q}} = \begin{cases} \sum_{\zeta \in \{1, \dots, p\}, \zeta \neq \mathbf{q}} U_\zeta^{\mathbf{q}} - U_j^{\mathbf{q}}, & \text{for } i = \mathbf{q}, j \neq \mathbf{q} \\ \sum_{\zeta \in \{1, \dots, p\}, \zeta \neq \mathbf{q}} U_\zeta^{\mathbf{q}} - U_i^{\mathbf{q}}, & \text{for } i \neq \mathbf{q}, j = \mathbf{q} \\ -(U_i^{\mathbf{q}} + U_j^{\mathbf{q}}), & \text{for } i \neq \mathbf{q}, j \neq \mathbf{q} \end{cases}$$

with $\psi_{11} = (A_i X + B_i Y_j^{\mathbf{q}})^*$, $\psi_{13} = X F_i^T + Y_j^{\mathbf{q}T} G_i^T$, $\varphi_{12} = \mathbf{a}X + A_i X + B_i Y_j^{\mathbf{q}}$. Then, the gain matrices of controller (13) are calculated by $K_j^{\mathbf{q}} = Y_j^{\mathbf{q}} X^{-1}$.

Poof: Constructing the Lyapunov function as

$$V(t) = x^T(t) P x(t) \quad (25)$$

Then, it is obtained that

$$\dot{V} + z^T z - \gamma^2 \omega^T \omega = \xi^T \begin{bmatrix} (P\mathbf{A})^* + \mathbf{F}^T \mathbf{F} & P\mathbf{E} \\ * & -\gamma^2 I \end{bmatrix} \xi \quad (26)$$

where $\xi^T = [x^T \ \omega^T]$, $\mathbf{A} = A(\eta) + B(\eta)K^{\mathbf{q}}(\eta)$, $\mathbf{E} = E(\eta)$, $\mathbf{F} = F(\eta) + G(\eta)K^{\mathbf{q}}(\eta)$, with $[A \ B \ E \ F \ G] = \sum_{i=1}^p \eta_i(\varepsilon) [A_i \ B_i \ E_i \ F_i \ G_i]$. Due to the MFs $\eta_i \geq 0$, it is obtained from (21) and (22) that $\eta_i \eta_i (\Psi_{ii}^{\mathbf{q}} + \Pi_i^{\mathbf{q}}) \leq 0$ and $\eta_i \eta_j (\Psi_{ij}^{\mathbf{q}} + \Psi_{ji}^{\mathbf{q}} + \hat{\Pi}_{ij}^{\mathbf{q}}) \leq 0$. Then, it can be obtained that

$$\begin{aligned} & \sum_{i=1}^p \sum_{i=1}^p \eta_i \eta_i (\Psi_{ii}^{\mathbf{q}} + \Pi_i^{\mathbf{q}}) + \sum_{i=1}^p \sum_{i < j}^p \eta_i \eta_j (\Psi_{ij}^{\mathbf{q}} + \Psi_{ji}^{\mathbf{q}} + \hat{\Pi}_{ij}^{\mathbf{q}}) \\ &= \sum_{i=1}^p \sum_{i=1}^p \eta_i \eta_i \Psi_{ii}^{\mathbf{q}} + \sum_{i=1}^p \sum_{i < j}^p \eta_i \eta_j (\Psi_{ij}^{\mathbf{q}} + \Psi_{ji}^{\mathbf{q}}) \\ &+ \sum_{i=1}^p \sum_{i=1}^p \eta_i \eta_i \Pi_i^{\mathbf{q}} + \sum_{i=1}^p \sum_{i < j}^p \eta_i \eta_j \hat{\Pi}_{ij}^{\mathbf{q}} \\ &= \sum_{i=1}^p \sum_{j=1}^p \eta_i \eta_j \Psi_{ij}^{\mathbf{q}} + \sum_{j \in \{1, \dots, p\}, j \neq \mathbf{q}} (\eta_{\mathbf{q}} - \eta_j) Q_j^{\mathbf{q}} \leq 0 \end{aligned} \quad (27)$$

Then, it follows that $\sum_{j \in \{1, \dots, p\}, j \neq \mathbf{q}} (\eta_{\mathbf{q}} - \eta_j) Q_j^{\mathbf{q}} > 0$, and

$$\sum_{i=1}^p \sum_{j=1}^p \eta_i \eta_j \Psi_{ij}^{\mathbf{q}} = \begin{bmatrix} \tilde{\psi}_{11} & \tilde{\psi}_{12} & \tilde{\psi}_{13} \\ * & \tilde{\psi}_{22} & 0 \\ * & * & -I \end{bmatrix} \leq 0 \quad (28)$$

where $\tilde{\psi}_{11} = (AX + BY^{\mathbf{q}})^*$, $\tilde{\psi}_{12} = E$, $\tilde{\psi}_{13} = XF^T + Y^{\mathbf{q}T} G^T$, $\tilde{\psi}_{22} = -\gamma^2 I$. Next, let $P = X^{-1}$, multiply the left and right ends of the equation (28) by the matrix $\text{diag}\{P, I, I\}$ and its transpose, and then using Schur Lemma, it is obtained that $\dot{V}(t) + z^T(t)z(t) - \gamma^2 \omega^T(t)\omega(t) \leq 0$. Then, it follows that

$$V(\infty) - V(0) + \int_0^\infty z^T(t)z(t)dt - \gamma^2 \int_0^\infty \omega^T(t)\omega(t)dt \leq 0 \quad (29)$$

Due to $V(\infty) \geq 0$, under the zero initial condition, it follows that $\int_0^\infty z^T z dt \leq \gamma^2 \int_0^\infty \omega^T \omega dt$. Using a similar idea of the condition (27), one can get

$$\sum_{i=1}^p \sum_{j=1}^p \eta_i \eta_j \Upsilon_{ij}^{\mathbf{q}} = \begin{bmatrix} -\mathbf{r}X & \mathbf{a}X + \mathbf{A}X \\ * & -\mathbf{r}X \end{bmatrix} \leq 0 \quad (30)$$

By the Lemma 1, this proof is completed.

In the absence of DoS attacks, the fuzzy controller without switching mechanism can be used to ensure the stability of the system through the following corollary.

COROLLARY 1. For given scalars $\gamma > 0$, $\ell_g > 0$, $\mathfrak{R} > 0$, \mathbf{a} , \mathbf{r} , the system (11) under controller (15) is \mathcal{D} -stable with the H_∞ level, if there exists matrices $X > 0$, Y_j , such that

$$\tilde{\Psi}_{ii} < 0, \text{ for } i \in \{1, 2, \dots, p\} \quad (31)$$

$$\tilde{\Psi}_{ij} + \tilde{\Psi}_{ji} < 0, \text{ for } 1 \leq i < j \leq p \quad (32)$$

$$\tilde{\Upsilon}_{ii} < 0, \text{ for } i \in \{1, 2, \dots, p\} \quad (33)$$

$$\tilde{\Upsilon}_{ij} + \tilde{\Upsilon}_{ji} < 0, \text{ for } 1 \leq i < j \leq p \quad (34)$$

where

$$\tilde{\Psi}_{ij} = \begin{bmatrix} \hat{\psi}_{11} & E_i & \hat{\psi}_{13} \\ * & -\gamma^2 I & 0 \\ * & * & -I \end{bmatrix}, \tilde{\Upsilon}_{ij} = \begin{bmatrix} -\mathbf{r}X & \hat{\varphi}_{12} \\ * & -\mathbf{r}X \end{bmatrix}$$

with $\hat{\psi}_{11} = (A_i X + B_i Y_j)^*$, $\hat{\psi}_{13} = X F_i^T + Y_j^T G_i^T$, $\hat{\varphi}_{12} = \mathbf{a}X + A_i X + B_i Y_j$. Then, the gains of controller (15) are obtained by $K_j = Y_j X^{-1}$.

Proof: The proof idea is similar to that of Theorem 1. Due to space reasons, the specific proof process is omitted.

F. LMI-Based Security Control Design under DoS attacks

In order to deal with DoS attacks, a novel fuzzy controller with switching is used, and the following theorem conditions are given to ensure the stability of the system.

THEOREM 2. For given scalars $\gamma > 0$, $\mu_g \geq 1$, $\lambda_g > 0$, $\ell_g > 0$, $\mathfrak{R} > 0$, \mathbf{a} and \mathbf{r} , the system (18) is exponentially stable with H_∞ performance $(\alpha, \bar{\gamma})$, if exists matrices $X_g > 0$ with $g \in \{1, 2\}$, $Y_j^{\mathbf{q}}$, additional matrices $O_\zeta^{\mathbf{q}} > 0$, $W_\zeta^{\mathbf{q}} > 0$, with $j, \mathbf{q}, \zeta \in \{1, \dots, p\}$, such that

$$\Phi_{1ii}^{\mathbf{q}} + H_i^{\mathbf{q}} < 0, \text{ for } i \in \{1, 2, \dots, p\} \quad (35)$$

$$\Phi_{1ij}^{\mathbf{q}} + \Phi_{1ji}^{\mathbf{q}} + \hat{H}_{ij}^{\mathbf{q}} < 0, \text{ for } 1 \leq i < j \leq p \quad (36)$$

$$\Phi_{2i}^{\mathbf{q}} < 0, \text{ for } i \in \{1, 2, \dots, p\} \quad (37)$$

$$\begin{bmatrix} -\mu_1 X_1 & X_1 \\ * & -X_2 \end{bmatrix} \leq 0, \begin{bmatrix} -\mu_2 X_2 & X_2 \\ * & -X_1 \end{bmatrix} \leq 0 \quad (38)$$

$$\varrho = \lambda_1 - \frac{\lambda_1 + \lambda_2}{T} - \frac{\ln \mu}{\tau_D} \geq 0 \quad (39)$$

$$\hat{\Upsilon}_{1ii}^{\mathbf{q}} + \Lambda_i^{\mathbf{q}} < 0, \text{ for } i \in \{1, 2, \dots, p\} \quad (40)$$

$$\hat{\Upsilon}_{1ij}^{\mathbf{q}} + \hat{\Upsilon}_{1ji}^{\mathbf{q}} + \hat{\Lambda}_{ij}^{\mathbf{q}} < 0, \text{ for } 1 \leq i < j \leq p \quad (41)$$

$$\hat{\Upsilon}_{2i}^{\mathbf{q}} < 0, \text{ for } i \in \{1, 2, \dots, p\} \quad (42)$$

where

$$\Phi_{1ij}^{\mathbf{q}} = \begin{bmatrix} \phi_{11} & E_i & \phi_{13} \\ * & -\gamma^2 I & 0 \\ * & * & -I \end{bmatrix}, \Phi_{2i}^{\mathbf{q}} = \begin{bmatrix} \check{\phi}_{11} & E_i & \check{\phi}_{13} \\ * & -\gamma^2 I & 0 \\ * & * & -I \end{bmatrix}$$

$$\hat{\Upsilon}_{1ij}^{\mathbf{q}} = \begin{bmatrix} -\mathbf{r}X_1 & \bar{\varphi}_{12} \\ * & -\mathbf{r}X_1 \end{bmatrix}, \hat{\Upsilon}_{2i}^{\mathbf{q}} = \begin{bmatrix} -\mathbf{r}X_2 & \check{\varphi}_{12} \\ * & -\mathbf{r}X_2 \end{bmatrix}$$

$$H_i^{\mathbf{q}} = \begin{cases} \sum_{\zeta \in \{1, \dots, p\}, \zeta \neq \mathbf{q}} O_\zeta^{\mathbf{q}}, & \text{for } i = \mathbf{q} \\ -O_i^{\mathbf{q}}, & \text{for } i \neq \mathbf{q} \end{cases}$$

$$\hat{H}_{ij}^{\mathbf{q}} = \begin{cases} \sum_{\zeta \in \{1, \dots, p\}, \zeta \neq \mathbf{q}} O_\zeta^{\mathbf{q}} - O_j^{\mathbf{q}}, & \text{for } i = \mathbf{q}, j \neq \mathbf{q} \\ \sum_{\zeta \in \{1, \dots, p\}, \zeta \neq \mathbf{q}} O_\zeta^{\mathbf{q}} - O_i^{\mathbf{q}}, & \text{for } i \neq \mathbf{q}, j = \mathbf{q} \\ -(O_i^{\mathbf{q}} + O_j^{\mathbf{q}}), & \text{for } i \neq \mathbf{q}, j \neq \mathbf{q} \end{cases}$$

$$\Lambda_i^{\mathbf{q}} = \begin{cases} \sum_{\zeta \in \{1, \dots, p\}, \zeta \neq \mathbf{q}} W_\zeta^{\mathbf{q}}, & \text{for } i = \mathbf{q} \\ -W_i^{\mathbf{q}}, & \text{for } i \neq \mathbf{q} \end{cases}$$

$$\hat{\Lambda}_{ij}^{\mathbf{q}} = \begin{cases} \sum_{\zeta \in \{1, \dots, p\}, \zeta \neq \mathbf{q}} W_\zeta^{\mathbf{q}} - W_j^{\mathbf{q}}, & \text{for } i = \mathbf{q}, j \neq \mathbf{q} \\ \sum_{\zeta \in \{1, \dots, p\}, \zeta \neq \mathbf{q}} W_\zeta^{\mathbf{q}} - W_i^{\mathbf{q}}, & \text{for } i \neq \mathbf{q}, j = \mathbf{q} \\ -(W_i^{\mathbf{q}} + W_j^{\mathbf{q}}), & \text{for } i \neq \mathbf{q}, j \neq \mathbf{q} \end{cases}$$

with $\phi_{11} = (A_i X_1 + B_i Y_j^{\mathbf{q}})^* + \lambda_1 X_1$, $\phi_{13} = X_1 F_i^T + Y_j^{\mathbf{q}T} G_i^T$, $\check{\phi}_{11} = (A_i X_2)^* - \lambda_2 X_2$, $\check{\phi}_{13} = X_2 F_i^T + Y_j^{\mathbf{q}T} G_i^T$, $\bar{\varphi}_{12} = \mathbf{a}X_1 + A_i X_1 + B_i Y_j^{\mathbf{q}}$, $\mu = \mu_1 \mu_2$, $\alpha = \frac{\ln \mu}{\tau_D}$, $\bar{\gamma} = \sqrt{\frac{\lambda_1 \mu_1 \mu_2 e^{(\lambda_1 + \lambda_2) \tau}}{\nu} \gamma^2}$, $\nu = \lambda_1 - \frac{\lambda_1 + \lambda_2}{T}$. Then, the controller gains can be obtained by $K_j^{\mathbf{q}} = Y_j^{\mathbf{q}} X_1^{-1}$.

Proof: Construct the piecewise Lyapunov function:

$$V(t) = \begin{cases} V_1(t), & t \in [h_{n-1} + \tau_{n-1}, h_n) \\ V_2(t), & t \in [h_n, h_n + \tau_n) \end{cases} \quad (43)$$

where $V_g(t) = x^T(t) P_g x(t)$, $g \in \{1, 2\}$. Then, when $g = 1$, $t \in [h_{n-1} + \tau_{n-1}, h_n)$, it is obtained that

$$\begin{aligned} & \dot{V}_1(t) + \lambda_1 V_1(t) + z^T(t) z(t) - \gamma^2 \omega^T(t) \omega(t) \\ & = \xi^T \begin{bmatrix} (P_1 \mathbf{A}_1^{\mathbf{q}})^* + \lambda_1 P_1 + \mathbf{F}_1^{\mathbf{q}T} \mathbf{F}_1^{\mathbf{q}} & P_1 E \\ * & -\gamma^2 I \end{bmatrix} \xi \end{aligned} \quad (44)$$

where $\mathbf{A}_1^{\mathbf{q}} = A(\eta) + B(\eta)K^{\mathbf{q}}(\eta)$, $\mathbf{F}_1^{\mathbf{q}} = F(\eta) + G(\eta)K^{\mathbf{q}}(\eta)$. Similar to formulas (27) and (29), it follows by conditions (35) and (36) that

$$\dot{V}_1(t) + \lambda_1 V_1(t) + z^T(t) z(t) - \gamma^2 \omega^T(t) \omega(t) \leq 0 \quad (45)$$

Similar derivation, when $g = 2$, when $t \in [h_n, h_n + \tau_n)$, it can be got from condition (37) that

$$\dot{V}_2(t) - \lambda_2 V_2(t) + z^T(t) z(t) - \gamma^2 \omega^T(t) \omega(t) \leq 0 \quad (46)$$

For the sake of analysis, we give the following symbol definition $\mathcal{I}_{l,n} = [t_{l,n}, t_{3-l,n+l-1}]$, where

$$t_{l,n} = \begin{cases} h_{n-1} + \tau_{n-1}, & l = 1 \\ h_n, & l = 2 \end{cases}$$

By the condition (38) and (43), it can be got

$$V_1(t_{1,n}) \leq \mu_2 V_2(t_{1,n}^-), V_2(t_{2,n}) \leq \mu_1 V_1(t_{2,n}^-) \quad (47)$$

Then, when $\omega = 0$, $t \in \mathcal{I}_{1,n}$, it is obtained that

$$\begin{aligned} V(t) &\leq e^{-\lambda_1(t-t_{1,n})} V_1(t_{1,n}) \\ &\leq \mu_2 e^{-\lambda_1(t-t_{1,n})} V_2(t_{1,n}^-) \\ &\leq \mu^{n(0,t)} e^{-\lambda_1|\Theta(0,t)|} e^{\lambda_2|\Xi(0,t)|} V_1(0) \\ &\leq \mu^{\left(\epsilon + \frac{t}{\tau_D}\right)} e^{-\lambda_1(t-\kappa - \frac{t}{T})} e^{\lambda_2(\kappa - \frac{t}{T})} V_1(0) \\ &\leq \mathbf{M}_1 e^{-\rho t} V_1(0) \end{aligned} \quad (48)$$

where $\mathbf{M}_1 = e^{(\epsilon \ln \mu + \lambda_1 \kappa + \lambda_2 \kappa)}$ and $\rho = \lambda_1 - \frac{\lambda_1 + \lambda_2}{T} - \frac{\ln \mu}{\tau_D}$. Then, when $t \in \mathcal{I}_{2,n}$, using a similar derivation as in (48), it is obtained that

$$\begin{aligned} V(t) &\leq e^{\lambda_2(t-t_{2,n})} V_2(t_{2,n}) \\ &\leq \frac{1}{\mu_2} \mu^{\left(\epsilon + \frac{t}{\tau_D}\right)} e^{-\lambda_1(t-\kappa - \frac{t}{T})} e^{\lambda_2(\kappa - \frac{t}{T})} V_1(0) \\ &\leq \mathbf{M}_2 e^{-\rho t} V_1(0) \end{aligned} \quad (49)$$

where $\mathbf{M}_2 = \frac{e^{(\epsilon \ln \mu + \lambda_1 \kappa + \lambda_2 \kappa)}}{\mu_2}$. Combining (48) and (49), it is follows that $V(t) \leq \mathbf{M} e^{-\rho t} V_1(0)$, where $\mathbf{M} = \max\{\mathbf{M}_1, \mathbf{M}_2\}$. Base on the definition of $V(t)$, one can deduce that $V(t) \geq \hat{\alpha}_1 \|x(t)\|^2$, $V_1(0) \leq \hat{\alpha}_2 \mathbf{M} \|x(0)\|^2$. Then, it is can be got $\|x(t)\| \leq \sqrt{\frac{\hat{\alpha}_2 \mathbf{M}}{\hat{\alpha}_1}} e^{-\frac{\rho}{2} t} \|x(0)\|$, where $\hat{\alpha}_1 = \min\{\lambda_{\min}\{P_g\}\}$ and $\hat{\alpha}_2 = \lambda_{\max}\{P_1\}$. Then, the system (18) is exponentially stable. Next, consider the case of $\omega \neq 0$, when $t \in \mathcal{I}_{1,n}$, it is obtained that

$$\begin{aligned} V(t) &\leq \mu_2 e^{-\lambda_1(t-t_{1,n})} \left[e^{\lambda_2(t_{1,n}-t_{2,n-1})} V_2(t_{2,n-1}) \right. \\ &\quad \left. - \int_{t_{2,n-1}}^{t_{1,n}} e^{\lambda_2(t_{1,n}-s)} \mathbf{H} ds \right] - \int_{t_{1,n}}^t e^{-\lambda_1(t-s)} \mathbf{H} ds \\ &\leq \mathcal{H} - \sum_{i=1}^{n(0,t)} \mu^i \int_{t_{1,n-i}}^{t_{2,n-i}} \bar{\Gamma} \mathbf{H} ds \\ &\quad - \sum_{i=1}^{n(0,t)} \frac{\mu^i}{\mu_1} \int_{t_{2,n-i}}^{t_{1,n-i+1}} \bar{\Gamma} \mathbf{H} ds - \int_{t_{1,n}}^t \bar{\Gamma} \mathbf{H} ds \end{aligned} \quad (50)$$

where $\mathcal{H} = \mu^{n(0,t)} \Gamma V_1(0)$, $\Gamma = e^{-\lambda_1|\Theta(0,t)|} e^{\lambda_2|\Xi(0,t)|}$, $\bar{\Gamma} = e^{-\lambda_1|\Theta(s,t)| + \lambda_2|\Xi(s,t)|}$, $\mathbf{H} = z(s)^T z(s) - \gamma^2 \omega(s)^T \omega(s)$. Then, when $\omega \neq 0$, $t \in \mathcal{I}_{2,n}$, it is obtained that

$$\begin{aligned} V(t) &\leq e^{\lambda_2(t-t_{2,n})} V_2(t_{2,n}) - \int_{t_{2,n}}^t e^{\lambda_2(t-s)} \mathbf{H} ds \\ &\leq \frac{1}{\mu_2} \mathcal{H} - \sum_{i=1}^{n(0,t)} \frac{\mu^i}{\mu_2} \int_{t_{1,n-i+1}}^{t_{2,n-i+1}} \bar{\Gamma} \mathbf{H} ds \\ &\quad - \sum_{i=2}^{n(0,t)} \frac{\mu^i}{\mu} \int_{t_{2,n-i+1}}^{t_{1,n-i+2}} \bar{\Gamma} \mathbf{H} ds - \int_{t_{2,n}}^t \bar{\Gamma} \mathbf{H} ds \end{aligned} \quad (51)$$

Then, it can be obtained from (50) that

$$\begin{aligned} V(t) &\leq \mathcal{H} - \sum_{i=1}^{n(0,t)} \int_{t_{1,n-i}}^{t_{2,n-i}} \hat{\Gamma} ds \\ &\quad - \sum_{i=1}^{n(0,t)} \frac{1}{\mu_1} \int_{t_{2,n-i}}^{t_{1,n-i+1}} \hat{\Gamma} ds - \int_{t_{1,n}}^t \hat{\Gamma} ds \end{aligned} \quad (52)$$

where $\hat{\Gamma} = e^{n(s,t) \ln \mu} \bar{\Gamma} \mathbf{H}$. Then, it is can be obtained from (51) that

$$\begin{aligned} V(t) &\leq \frac{1}{\mu_2} \mathcal{H} - \sum_{i=1}^{n(0,t)} \int_{t_{1,n-i+1}}^{t_{2,n-i+1}} \frac{1}{\mu_2} \hat{\Gamma} ds \\ &\quad - \sum_{i=2}^{n(0,t)} \frac{1}{\mu} \int_{t_{2,n-i+1}}^{t_{1,n-i+2}} \hat{\Gamma} ds - \int_{t_{2,n}}^t \frac{1}{\mu} \hat{\Gamma} ds \end{aligned} \quad (53)$$

By the fact that $V(t) \geq 0$, (52) and zero initial conditions that

$$\begin{aligned} &\sum_{i=1}^{n(0,t)} \int_{t_{1,n-i}}^{t_{2,n-i}} \Delta ds + \sum_{i=1}^{n(0,t)} \frac{1}{\mu_1} \int_{t_{2,n-i}}^{t_{1,n-i+1}} \Delta ds + \int_{t_{1,n}}^t \Delta ds \\ &\leq \gamma^2 \left[\sum_{i=1}^{n(0,t)} \int_{t_{1,n-i}}^{t_{2,n-i}} \bar{\Delta} ds + \sum_{i=1}^{n(0,t)} \frac{1}{\mu_1} \int_{t_{2,n-i}}^{t_{1,n-i+1}} \bar{\Delta} ds \right. \\ &\quad \left. + \int_{t_{1,n}}^t \bar{\Delta} ds \right] \end{aligned} \quad (54)$$

where $\Delta = e^{n(s,t)} \bar{\Gamma} z^T z$, $\bar{\Delta} = e^{n(s,t)} \bar{\Gamma} \omega^T \omega$ which implies

$$\frac{1}{\mu_1} \int_0^t \Delta ds \leq \gamma^2 \int_0^t \bar{\Delta} ds \quad (55)$$

Multiplying the inequality in (55) by $e^{-n(0,t) \ln \mu}$ yields

$$\frac{1}{\mu_1} \int_0^t e^{-n(0,s) \ln \mu} \bar{\Gamma} z^T z ds \leq \gamma^2 \int_0^t e^{-n(0,s) \ln \mu} \bar{\Gamma} \omega^T \omega ds \quad (56)$$

Then, by $V(t) \geq 0$, (53) and zero initial conditions, it can be obtained the same equation (56). It can be obtained by Assumptions 1 and 2 that

$$-\lambda_1 |\Theta(s,t)| + \lambda_2 |\Xi(s,t)| \leq \bar{\mathcal{G}} \quad (57)$$

and

$$-\lambda_1 |\Theta(s,t)| + \lambda_2 |\Xi(s,t)| - n(0,s) \ln \mu \geq \mathcal{G} \quad (58)$$

where $\bar{\mathcal{G}} = (\lambda_1 + \lambda_2) \kappa + \left(\frac{\lambda_1 + \lambda_2}{T} - \lambda_1\right) (t-s)$, $\mathcal{G} = -\lambda_1(t-s) - \left(\frac{s}{\tau_D} + \epsilon\right) \ln \mu$. Then, it follows that

$$\int_0^t e^{\mathcal{G}} z^T z ds \leq \mu_1 \gamma^2 \int_0^t e^{\bar{\mathcal{G}}} \omega^T \omega ds \quad (59)$$

where $\bar{\mathcal{G}} = (\lambda_1 + \lambda_2) \kappa + \left(\frac{\lambda_1 + \lambda_2}{T} - \lambda_1\right) (t-s)$. Then, it follows that

$$\int_0^\infty e^{-\alpha s} z^T z ds \leq \bar{\gamma}^2 \int_0^\infty \omega^T \omega ds \quad (60)$$

where $\alpha = \frac{\ln \mu}{\tau_D}$, $\bar{\gamma} = \sqrt{\frac{\lambda_1 \mu^\epsilon \mu_1 \gamma^2 e^{(\lambda_1 + \lambda_2) \kappa}}{\nu}}$, and $\nu = \lambda_1 - \frac{\lambda_1 + \lambda_2}{T}$. Then, it is can be obtained from (40) and (41) that

$$\sum_{i=1}^p \sum_{j=1}^p \eta_i \eta_j \tilde{\Gamma}_{1ij}^{\mathbf{a}} = \begin{bmatrix} -\mathbf{r} X_1 & \mathbf{a} X_1 + \mathbf{A}_1^{\mathbf{a}} X_1 \\ * & -\mathbf{r} X_1 \end{bmatrix} \leq 0 \quad (61)$$

and

$$\sum_{i=1}^p \eta_i \tilde{\Gamma}_{2i}^{\mathbf{a}} = \begin{bmatrix} -\mathbf{r} X_2 & \mathbf{a} X_2 + \mathbf{A}_2^{\mathbf{a}} X_2 \\ * & -\mathbf{r} X_2 \end{bmatrix} \leq 0 \quad (62)$$

where $\mathbf{A}_2^{\mathbf{a}} = A(\eta)$. By the Lemma 1, the proof is completed.

When a traditional T-S fuzzy controller is used to deal with DoS attacks, the following corollary can be used to ensure the stability of the system.

COROLLARY 2. *For given scalars $\gamma > 0$, $\mu_g \geq 1$, $\lambda_g > 0$, $\ell_g > 0$, $\Re > 0$, the system (11) under controller (15) is exponentially stable with H_∞ performance $(\alpha, \bar{\gamma})$, if exists matrices $X_g > 0$ with $g \in \{1, 2\}$, Y_j with $j \in \{1, \dots, p\}$, satisfying the condition (38), (39) and*

$$\tilde{\Phi}_{ii}^1 < 0, \text{ for } i \in \{1, 2, \dots, p\} \quad (63)$$

$$\tilde{\Phi}_{ij}^1 + \tilde{\Phi}_{ji}^1 < 0, \text{ for } 1 \leq i < j \leq p \quad (64)$$

$$\tilde{\Phi}_i^2 < 0, \text{ for } i \in \{1, 2, \dots, p\} \quad (65)$$

where

$$\tilde{\Phi}_{ij}^1 = \begin{bmatrix} \check{\phi}_{11} & E_i & \check{\phi}_{13} \\ * & -\gamma^2 I & 0 \\ * & * & -I \end{bmatrix}, \tilde{\Phi}_i^2 = \begin{bmatrix} \check{\phi}_{11} & E_i & \check{\phi}_{13} \\ * & -\gamma^2 I & 0 \\ * & * & -I \end{bmatrix}$$

with $\check{\phi}_{11} = (A_i X_1 + B_i Y_j)^* + \lambda_1 X_1$, $\check{\phi}_{13} = (A_i X_2)^* - \lambda_2 X_2$, $\check{\phi}_{13} = X_1 F_i^T + Y_j^T G_i^T$, $\check{\phi}_{13} = X_2 F_i^T$, $\nu = \lambda_1 - \frac{\lambda_1 + \lambda_2}{T}$, $\bar{\gamma} = \sqrt{\frac{\lambda_1 \mu_1 \mu^\epsilon e^{(\lambda_1 + \lambda_2) \kappa}}{\nu}} \gamma^2$. Then, the gains of controller can be obtained by $K_j = Y_j X_1^{-1}$.

Poof: It can be proved by a similar idea to the proof of Theorem 2, and the specific process is omitted due to the length of the paper.

IV. NUMERICAL SIMULATION

In this section, the vehicle simulation test platform built by CarSim and Matlab/Simulink is used to verify the effectiveness of the proposed scheme, as shown in Fig. 3. The advantages of the proposed scheme in tracking accuracy and driving comfort will be illustrated from three aspects: the comparison of H_∞ performance, the tracking performance of the vehicle, and the quantitative analysis of the vehicle tracking performance.

A. Comparison of H_∞ Performance under Different Methods

Without loss of generality, let $p = 2$, using the C-class vehicle model in CarSim and the correlation parameters are set as follows: $v_{x \min} = 18[km/h]$, $v_{x \max} = 72[km/h]$, $C_f = 107610[N/rad]$, $C_r = 74520[N/rad]$, $l_f = 1.015[m]$, $M = 1412[kg]$, $l_r = 1.895[m]$, $x_p = 5[m]$, $I_z = 1536.7[kgm^2]$. Then, the above parameters are brought into (10) to obtain the corresponding matrices A_i , B_i , E_i , F and G , where $i \in \{1, 2\}$. Next, based on Theorem 1 and Corollary 1, the numerical comparison as shown in Table II is obtained.

By comparing the data in Table II, it can be seen that with the same parameter value $\mathcal{D}(\mathbf{a}, \mathbf{r})$, the performance indicator $\gamma_{\min}^{Thm1} < \gamma_{\min}^{Cor1}$. Therefore, it can be found that the action of the switching mechanism, the solving constraint of Theorem 1 condition can be relaxed. Theorem 1 is less conservative than Corollary 1. This makes it possible to improve the vehicle tracking performance.

TABLE II
 H_∞ PERFORMANCE INDICATOR

Condition	Switching mechanism	\mathbf{a}	\mathbf{r}	γ_{\min}
Corollary 1	no	0.12	27.39	9.95
Theorem 1	yes	0.12	27.39	9.90
Corollary 1	no	0.12	26.39	10.74
Theorem 1	yes	0.12	26.39	10.61
Corollary 1	no	0.22	26	11.06
Theorem 1	yes	0.22	26	10.89

B. Analysis of Tracking Performance under Different Methods

To better demonstrate the advantages of our control scheme in terms of tracking accuracy and driving comfort, we compare Theorem 1, Corollary 1, Theorem 2, and Corollary 2 below. By comparison, the influence of the switching mechanism on the control scheme is explained in turn when there are no DoS attacks and when there are DoS attacks. The specific implementation process is as follows:

Firstly, the vehicle tracking test conditions are set in CarSim. Fig. 4 (a) shows the target path that the vehicle needs to track. The blue line in Fig. 4 (b) denotes the changing vehicle speed over time. The other line in Fig. 4 (b) denotes the curvature of the target path. As you can see from Fig. 4, the target path includes both curves and straights. The vehicle takes into account acceleration, deceleration, and uniform speed. The combination of target path and vehicle speed can make the simulation take into account most test scenarios, which is conducive to improving the persuasive power of the simulation.

Secondly, the corresponding controller gains are obtained by using Theorem 1, Corollary 1, Theorem 2, and Corollary 2 in turn. Without loss of generality, let $p = 2$, $\ell_1 = \ell_2 = \Re = 1$, and $\mathbf{r} = 48$, using the same vehicle parameter settings as above. It can be got from the Theorem 1 that

$$\begin{aligned} K_1^1 &= [-3.1891 \quad -0.0966 \quad -3.6621 \quad 9.6302], \\ K_2^1 &= [-6.9455 \quad -0.0965 \quad -6.3929 \quad 16.3290], \\ K_1^2 &= [-5.1517 \quad -0.1020 \quad -5.1497 \quad 13.1965], \\ K_2^2 &= [-5.6913 \quad -0.2187 \quad -5.7286 \quad 14.5500]. \end{aligned}$$

Then, by Corollary 1, under the same parameters in Theorem 1, the control gains are computed as

$$\begin{aligned} K_1 &= [-2.6360 \quad -0.1230 \quad -3.3279 \quad 8.5553], \\ K_2 &= [-5.5148 \quad -0.2188 \quad -5.4793 \quad 13.5989]. \end{aligned}$$

Without loss of generality, let $p = 2$, $\ell_1 = 0.1$, $\ell_2 = 0.1$, $\Re = 0.5$, $\lambda_1 = 2.1$, $\lambda_2 = 16$, $\mu_1 = \mu_2 = 1.01$, $\tau_D = 15$, $\mathbf{r} = 48.2$, $\mathbf{a} = 1$, and the same vehicle parameter as above. It can be computed from Theorem 2 that

$$\begin{aligned} K_1^1 &= [-0.4625 \quad -0.0221 \quad -1.2407 \quad 3.9364], \\ K_2^1 &= [-2.2763 \quad -0.0419 \quad -2.4068 \quad 7.5358], \\ K_1^2 &= [-0.5931 \quad 0.0032 \quad -1.3004 \quad 4.1531], \\ K_2^2 &= [-2.8413 \quad -0.0837 \quad -2.7997 \quad 8.6639]. \end{aligned}$$

Meanwhile, under the same parameters in Theorem 2, solving Corollary 2 yields the following gains:

$$\begin{aligned} K_1 &= [-21.5032 \quad 0.0852 \quad -11.7230 \quad 36.0220], \\ K_2 &= [-6.3955 \quad -0.2223 \quad -4.5154 \quad 13.9940]. \end{aligned}$$

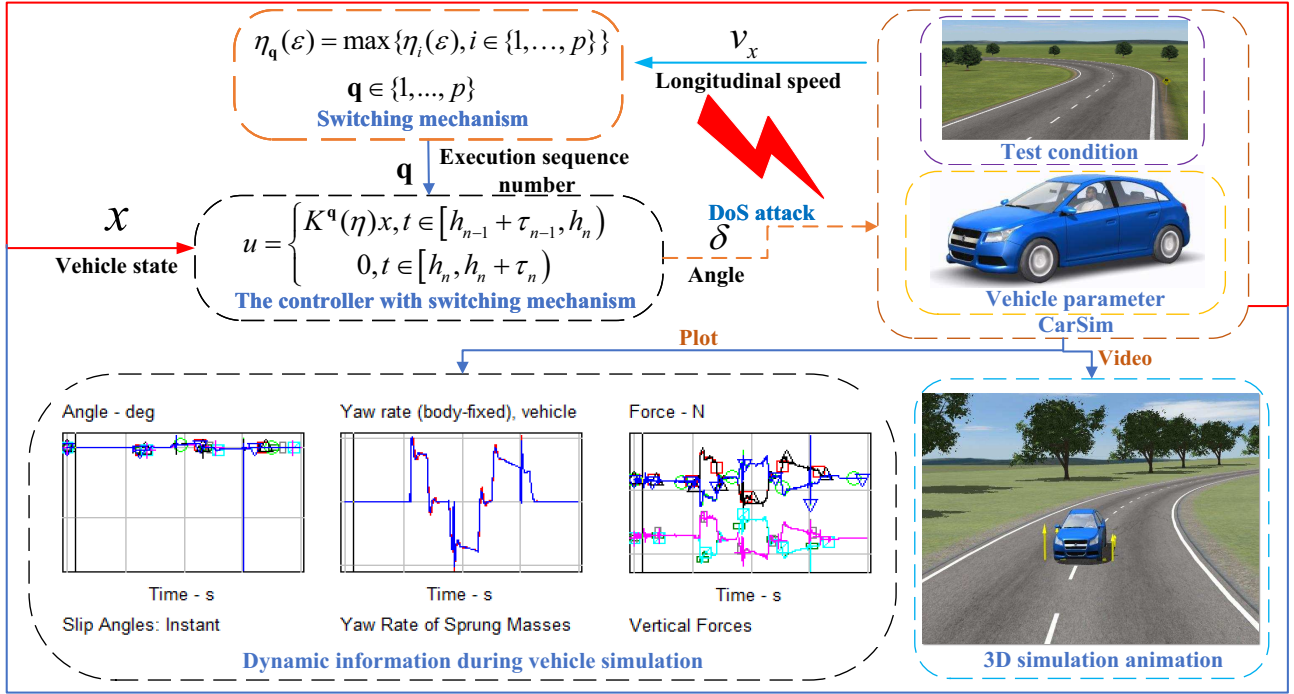


Fig. 3. Illustration of the test platform built by Matlab/Simulink and CarSim

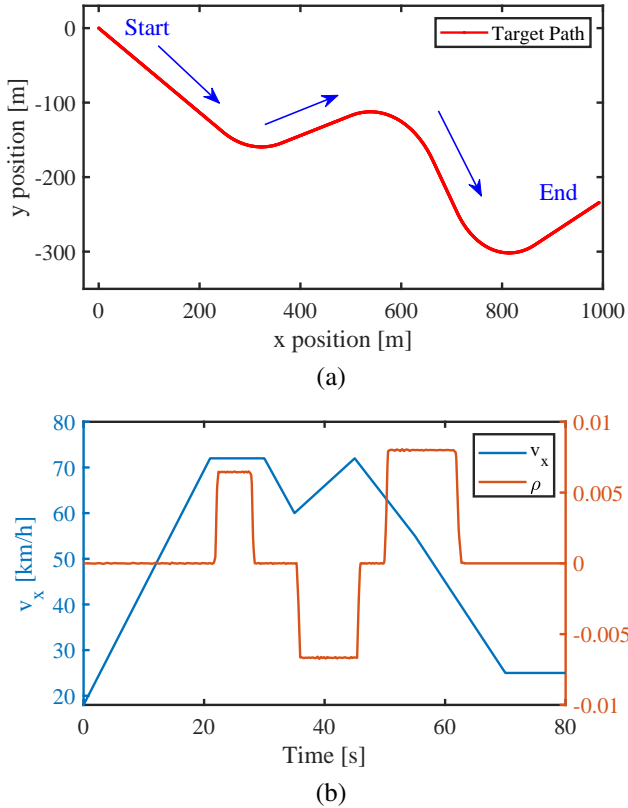


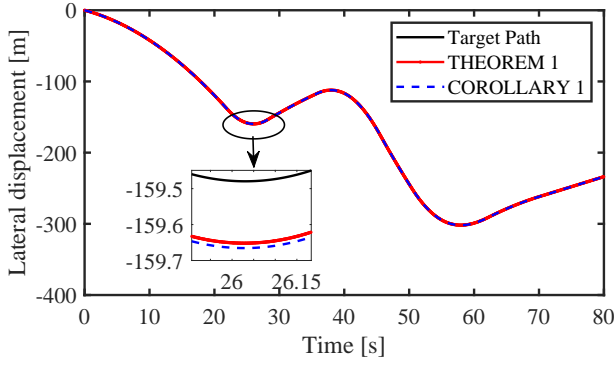
Fig. 4. Working condition of vehicle tracking. (a) Target path. (b) Path curvature ρ and vehicle speed v_x .

Thirdly, put the above controller gains into the simulation platform in Fig. 3 and obtain the tracking effect figures Fig. 5, 6, 7, 8, and 9 successively. Fig. 5 shows the situation

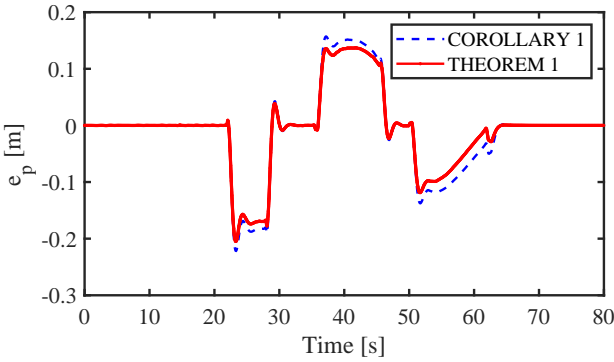
of path tracking without DoS attacks. From Fig. 5, the path tracking task can be completed under Theorem 1 condition and Corollary 1 condition. By enlarging some of the details in Fig. 5 (a), we can see that Theorem 1 has an advantage over Corollary 1 in cornering. Meanwhile, it can also found from Fig. 5 (b) that under the condition of Theorem 1, the vehicle is better able to handle corners and has better tracking accuracy. From this, we can conclude that without DoS attacks, Theorem 1 has better tracking control performance.

Fig. 6 shows the tracking effect with DoS attacks. DoS attacks sequence generated using a similar method as in [27] is adopted. Based on the above scalars τ_D , T , and $\epsilon = \kappa = 1$, it is obtained from Assumption 1 that $n(0, 80) < 6.33$. Also, it can be obtained from Assumption 2 that $|\Xi(0, 80)| < 4.10$. Due to the existence of DoS attacks, a part of the uncontrolled state will be generated, so the partial error in Fig. 6 (b) will be larger than that in Fig. 5 (b). But under the same conditions, Theorem 2 has a smaller e_p than Corollary 2. From Fig. 6 (b), it can be found that the gap between Theorem 2 and Corollary 2 is larger than the gap between Theorem 1 and Corollary 1. This further demonstrates that the switching mechanism is more advantageous in the face of DoS attacks.

Fig. 7 shows the dynamic information changes in the path tracking process, which can reflect the driving comfort in the process of vehicle tracking to a certain extent. Fig. 7 (a) and (b) show the δ and r without DoS attacks. From Fig. 7, it can be seen that the changes of δ and r under Theorem 1 and Corollary 1 are close, and the difference between the two is mainly reflected in the vehicle passing the corner. Due to the action of the switching mechanism, the vehicle responds more quickly when turning. Therefore, our control scheme has more advantages in tracking accuracy and driving experience.

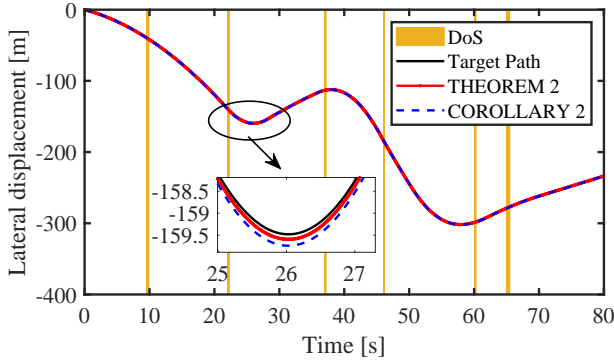


(a)

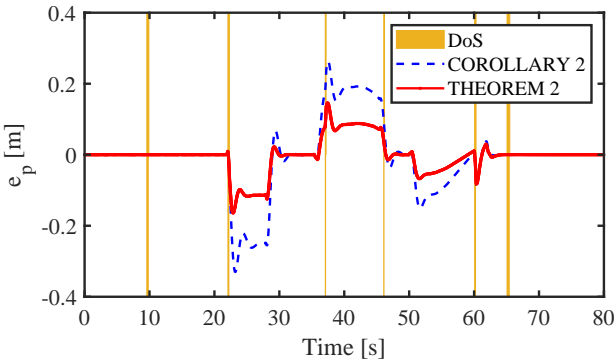


(b)

Fig. 5. Lateral displacement and e_p of the vehicle not subjected to DoS attacks under different stability conditions. (a) Displacement. (b) Lateral error e_p .

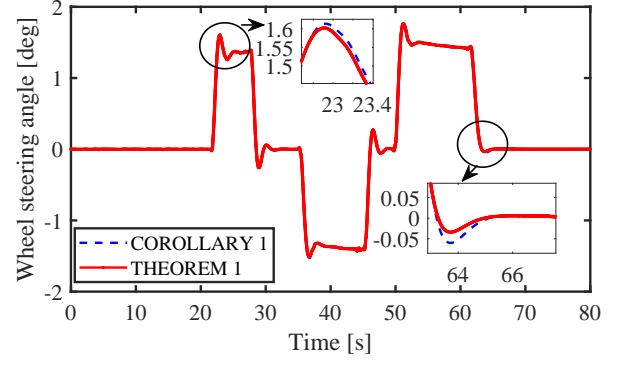


(a)

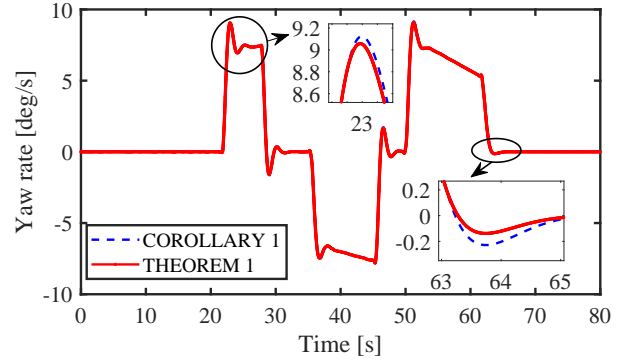


(b)

Fig. 6. Lateral displacement and e_p of the vehicle subjected to DoS attacks under different stability conditions. (a) Displacement. (b) Lateral error e_p .



(a)



(b)

Fig. 7. Steering angle δ and r of the vehicle not subjected to DoS attacks under different stability conditions. (a) δ . (b) r .

Fig. 8 (a) and (b) show the δ and r with DoS attacks. According to Fig. 8, it can also be found that in the face of DoS attacks, under the condition of Theorem 2, the change of δ and r is faster, and thus has a better effect. In particular, after magnifying the details in Fig. 8, it can be found that under the control of Theorem 2, the dynamic information of the vehicle tends to be stable more quickly after the DoS attacks and after passing the bend, indicating that the controller under Theorem 2 works stably, so that the vehicle can better cope with the influence of the DoS attacks and ensure its tracking accuracy.

Fig. 9 shows the β during the tracking process. Fig. 9 (a) does not consider the DoS attacks. Fig. 9 (b) considers the DoS attacks. It can be seen from Fig. 9 that the effect under Theorem 1 and Corollary 1 is close. However, the detailed control of the vehicle is better under our control scheme. In summary, using our control scheme, the tracking accuracy and driving experience of the vehicle are better.

C. Quantitative Analysis of Vehicle Tracking Performance

In this section, the advantages of our algorithm are further explained through quantitative analysis. In Tab. III, e_{pRMS} denotes the RMS value, e_{pMAE} denotes the MAE value, $|e_p|$ denotes the absolute value. $|e_p|_{\max}$ denotes the maximum value of the $|e_p|$. The smaller the $|e_p|_{\max}$, it indicates that the better the overall control response of the vehicle in the tracking process, the stronger the ability to deal with curves and DoS attacks, and the higher the tracking accuracy. The

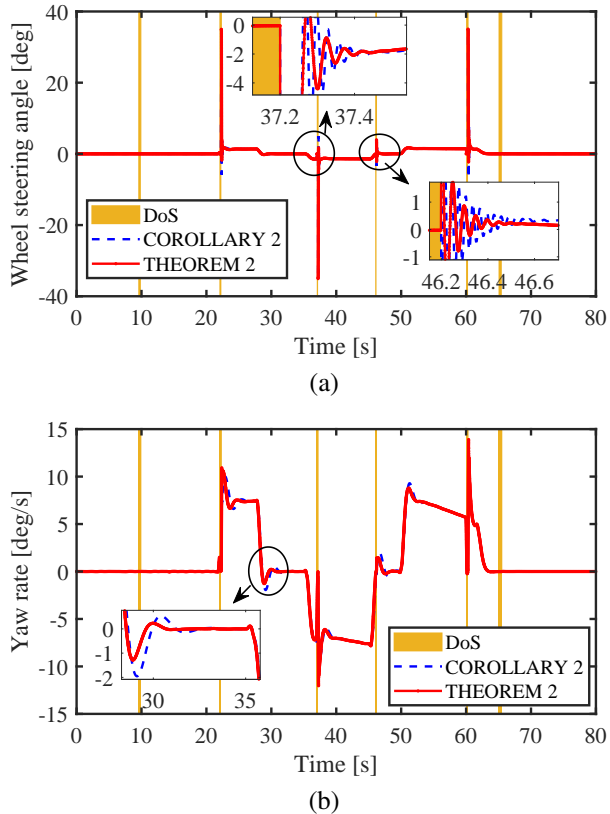


Fig. 8. Steering angle δ and r of the vehicle subjected to DoS attacks under different stability conditions. (a) δ . (b) r .

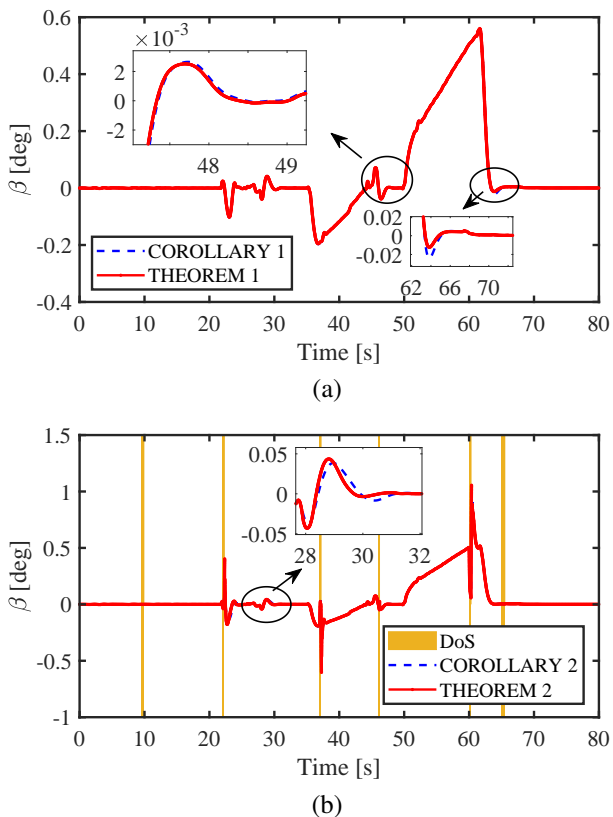


Fig. 9. Comparison of β under different stability conditions. (a) Without DoS attacks. (b) With DoS attacks.

smaller the e_{pRMS} and e_{pMAE} , the more comfortable and safe the driving is to a certain extent. Based on Table III, it can be found that the peak and fluctuation of the e_p of the Theorem condition with switching mechanism are better than those of the Corollary condition without switching mechanism. In particular, in the face of DoS attacks, the indices of Theorem 2 improve significantly. This once again validates the advantages of the switching mechanism in the rational use of vehicle dynamic information, delicate control and adjustment, and against DoS attacks.

TABLE III
VEHICLE PERFORMANCE ANALYSIS DURING PATH TRACKING

Condition	Switching mechanism	DoS	e_{pRMS}	e_{pMAE}	$ e_p _{max}$
Corollary 1	no	no	0.0792	0.0458	0.2220
Theorem 1	yes	no	0.0705	0.0395	0.2051
Corollary 2	no	yes	0.1007	0.0540	0.3304
Theorem 2	yes	yes	0.0471	0.0251	0.1644

To sum up, regardless of the existence of DoS attacks, our security control scheme, due to the use of the novel controller with a switching mechanism. It can better resist DoS attacks and cope with bends of unknown curvature, so as to ensure vehicle safety and tracking accuracy.

V. CONCLUSIONS

This paper, a new security control scheme is proposed to deal with the nonlinear AGV tracking control problem under no-periodic DoS attacks. Importantly, based on the normalized fuzzy membership functions, a novel fuzzy controller with a reasonable switching mechanism is designed. The fuzzy controller can be deployed according to the switching mechanism, so as to effectively deal with DoS attacks during vehicle driving. In addition, in order to be more suitable for practical applications, the idea of pole placement is used to improve the transient performance of the system to further ensure the safe driving and tracking accuracy of AGVs. The dynamic simulation examples under the Carsim-Matlab/Simulink co-simulation platform are used to illustrate the superiority of the proposed scheme. Finally, there are still some works to be explored in the future. More vehicle uncertainty information will be considered, and the tracking control problem of AGVs with tire force uncertainty/nonlinearity and other uncertain information will be studied. Moreover, in order to optimize the control performance, a new switching mechanism with a weighting coefficient will need to be developed. Third, but not the last, the tracking control of AGVs in complex network attack scenarios will be studied.

REFERENCES

- [1] J. E. A. Dias, G. A. S. Pereira and R. M. Palhares, "Longitudinal model identification and velocity control of an autonomous car," *IEEE Transactions on Intelligent Transportation Systems*, vol. 16, no. 2, pp. 776-786, 2015.
- [2] Z. Yang, J. Huang, D. Yang and Z. Zhong, "Design and optimization of robust path tracking control for autonomous vehicles with fuzzy uncertainty," *IEEE Transactions on Fuzzy Systems*, vol. 30, no. 6, pp. 1788-1800, 2022.

- [3] Y. Yu, J. Guo, M. Chadli and Z. Xiang, "Distributed adaptive fuzzy formation control of uncertain multiple unmanned aerial vehicles with actuator faults and switching topologies," *IEEE Transactions on Fuzzy Systems*, vol. 31, no. 3, pp. 919-929, 2023.
- [4] R. Marino, S. Scalzi and M. Netto, "Nested PID steering control for lane keeping in autonomous vehicles," *Control Engineering Practice*, vol. 19, no. 12, pp. 1459-1467, 2011.
- [5] W. Farag, "Complex trajectory tracking using PID control for autonomous driving," *International Journal of Intelligent Transportation Systems Research*, vol. 18, no. 2, pp. 356-366, 2020.
- [6] A. D. Sabiha, M. A. Kamel, E. Said and W. M. Hussein, "ROS-based trajectory tracking control for autonomous tracked vehicle using optimized backstepping and sliding mode control," *Robotics and Autonomous Systems*, vol. 152, 2022.
- [7] C. L. Hwang, C. C. Yang and J. Y. Hung, "Path tracking of an autonomous ground vehicle with different payloads by hierarchical improved fuzzy dynamic sliding-mode control," *IEEE Transactions on Fuzzy Systems*, vol. 26, no. 2, pp. 899-914, 2017.
- [8] A. Ferrara, G. P. Incremona and E. Regolin, "Optimization-based adaptive sliding mode control with application to vehicle dynamics control," *International Journal of Robust and Nonlinear Control*, vol. 29, no. 3, pp. 550-564, 2019.
- [9] R. M. Palhares and P. L. D. Peres, "LMI approach to the mixed H_2/H_∞ filtering design for discrete-time uncertain systems," *IEEE Transactions on Aerospace and Electronic Systems*, vol. 37, no. 1, pp. 292-296, 2001.
- [10] P. Hang, X. Chen and F. Luo, "LPV/ H_∞ controller design for path tracking of autonomous ground vehicles through four-wheel steering and direct yaw-moment control," *International Journal of Automotive Technology*, vol. 20, pp. 679-691, 2019.
- [11] R. M. Palhares and P. L. Peres, "Robust H_∞ filter design with pole constraints for discrete-time systems" *Journal of the Franklin Institute*, vol. 337, no. 6, pp. 713-723, 2000.
- [12] D. Q. Mayne, J. B. Rawlings, C. V. Rao and P. O. Scokaert, "Constrained model predictive control: Stability and optimality," *Automatica*, vol. 36, no. 6, pp. 789-814, 2000.
- [13] C. Shen, Y. Shi and B. Buckham, "Trajectory tracking control of an autonomous underwater vehicle using Lyapunov-based model predictive control," *IEEE Transactions on Industrial Electronics*, vol. 65, no. 7, pp. 5796-5805, 2017.
- [14] E. Alcalá, I. Bessa, V. Puig, O. Sename and R. Palhares, "MPC using an on-line TS fuzzy learning approach with application to autonomous driving," *Applied Soft Computing*, vol. 130, 109698, 2022.
- [15] P. Petrov and F. Nashashibi, "Modeling and nonlinear adaptive control for autonomous vehicle overtaking," *IEEE Transactions on Intelligent Transportation Systems*, vol. 15, no. 4, pp. 1643-1656, 2014.
- [16] A. Mohammadzadeh and H. Taghavifar, "A novel adaptive control approach for path tracking control of autonomous vehicles subject to uncertain dynamics," *Proceedings of the Institution of Mechanical Engineers, Part D: Journal of Automobile Engineering*, vol. 234, no. 8, pp. 2115-2126, 2020.
- [17] H. T. Sun, C. Peng and F. Ding, "Self-discipline predictive control of autonomous vehicles against denial of service attacks," *Asian Journal of Control*, vol. 24, no. 6, pp. 3538-3551, 2022.
- [18] F. Ding, H. Shan, X. Han, C. Jiang, C. Peng and J. Liu, "Security-based resilient triggered output feedback lane keeping control for Human-Machine cooperative steering intelligent heavy truck under Denial-of-Service attacks," *IEEE Transactions on Fuzzy Systems*, vol. 31, no. 7, pp. 2264-2276, 2023.
- [19] C. Deng, F. Meng, X. Xie, D. Yue, W. W. Che and S. Fan, "Data-driven based distributed fuzzy tracking control for nonlinear MASs under DoS attacks," *IEEE Transactions on Fuzzy Systems*, 2023.
- [20] S. K. Sah Tyagi, R. Yadav, D. K. Jain, Y. Tu and W. Zhang, "Paired swarm optimized relational vector learning for FDI attack detection in IoT-Aided smart grid," *IEEE Internet of Things Journal*, vol. 10, no. 21, pp. 18708-18717, 2023.
- [21] F. Yang, X. Xie and C. Peng, "Co-design of new fuzzy switching-type state-FDI estimation and attack compensation for DC microgrids under hybrid attacks," *IEEE Transactions on Fuzzy Systems*, 2023. Doi: 10.1109/TFUZZ.2023.3333314.
- [22] N. Nishanth and A. Mujeeb, "Modeling and detection of flooding-based denial-of-service attack in wireless Ad Hoc network using Bayesian inference," *IEEE Systems Journal*, vol. 15, no. 1, pp. 17-26, 2021.
- [23] P. S. Pessim, M. L. Peixoto, R. M. Palhares and M. J. Lacerda, "Static output-feedback control for cyber-physical LPV systems under DoS attacks," *Information Sciences*, vol. 563, pp. 241-255, 2021.
- [24] Y. Fan, X. Huang, Z. Wang, J. Xia and H. Shen, "Resilient sampled-data control for stabilization of T-S fuzzy systems via interval-dependent function method: handling DoS attacks," *IEEE Transactions on Fuzzy Systems*, vol. 31, no. 6, pp. 1830-1842, 2023.
- [25] P. H. S. Coutinho, I. Bessa, P. S. Pessim and R. M. Palhares, "A switching approach to event-triggered control systems under denial-of-service attacks," *Nonlinear Analysis: Hybrid Systems*, vol. 50, 101383, 2023.
- [26] W. Li, H. Du, Z. Feng, L. Deng, D. Ning and W. Li, "Stability analysis for H_∞ -controlled active quarter-vehicle suspension systems with a resilient event-triggered scheme under periodic DoS attacks," *IEEE Transactions on Cybernetics*, 2022.
- [27] Z. Gu, X. Sun, H. K. Lam, D. Yue and X. Xie, "Event-based secure control of T-S fuzzy-based 5-DOF active semivehicle suspension systems subject to DoS attacks," *IEEE Transactions on Fuzzy Systems*, vol. 30, no. 6, pp. 2032-2043, 2021.
- [28] Z. Lian, P. Shi, C. C. Lim and X. Yuan, "Fuzzy-model-based lateral control for networked autonomous vehicle systems under hybrid cyber-attacks," *IEEE Transactions on Cybernetics*, vol. 53, no. 4, pp. 2600-2609, 2022.
- [29] Y. Ma, Z. Nie, S. Hu, Z. Li, R. Malekian and M. Sotelo, "Fault detection filter and controller co-design for unmanned surface vehicles under DoS attacks," *IEEE Transactions on Intelligent Transportation Systems*, vol. 22, no. 3, pp. 1422-1434, 2020.
- [30] J. Wu, Q. Kong, K. Yang, Y. Liu, D. Cao and Z. Li, "Research on the steering torque control for intelligent vehicles co-driving with the penalty factor of human-machine intervention," *IEEE Transactions on Systems, Man, and Cybernetics: Systems*, vol. 53, no. 1, pp. 59-70, 2022.
- [31] A. T. Nguyen, C. Sentouh and J. C. Popieul, "Fuzzy steering control for autonomous vehicles under actuator saturation: Design and experiments," *Journal of the Franklin Institute*, vol. 355, no. 18, pp. 9374-9395, 2018.
- [32] A. T. Nguyen, T. Q. Dinh, T. M. Guerra and J. Pan, "Takagi-Sugeno fuzzy unknown input observers to estimate nonlinear dynamics of autonomous ground vehicles: Theory and real-time verification," *IEEE/ASME Transactions on Mechatronics*, vol. 26, no. 3, pp. 1328-1338, 2021.
- [33] C. Sentouh, A. T. Nguyen, M. A. Benloucif and J. C. Popieul, "Driver-automation cooperation oriented approach for shared control of lane keeping assist systems," *IEEE Transactions on Control Systems Technology*, vol. 27, no. 5, pp. 1962-1978, 2019.
- [34] R. Wang, H. Zhang and J. Wang, "Linear parameter-varying controller design for four-wheel independently actuated electric ground vehicles with active steering systems," *IEEE Transactions on Control Systems Technology*, vol. 22, no. 4, pp. 1281-1296, 2013.
- [35] H. O. Wang and K. Tanaka, "Fuzzy control systems design and analysis: a linear matrix inequality approach," *John Wiley and Sons*, 2004.
- [36] A. T. Nguyen, J. Rath, T. M. Guerra, R. Palhares and H. Zhang, "Robust set-invariance based fuzzy output tracking control for vehicle autonomous driving under uncertain lateral forces and steering constraints," *IEEE Transactions on Intelligent Transportation Systems*, vol. 22, no. 9, pp. 5849-5860, 2020.
- [37] X. Su, P. Shi, L. Wu and Y. D. Song, "Fault detection filtering for nonlinear switched stochastic systems," *IEEE Transactions on Automatic Control*, vol. 61, no. 5, pp. 1310-1315, 2015.
- [38] C. De Persis, and P. Tesi, "Input-to-state stabilizing control under denial-of-service," *IEEE Transactions on Automatic Control*, vol. 60, no. 11, pp. 2930-2944, 2015.
- [39] A. T. Nguyen, C. Sentouh, H. Zhang and J. C. Popieul, "Fuzzy static output feedback control for path following of autonomous vehicles with transient performance improvements," *IEEE Transactions on Intelligent Transportation Systems*, vol. 21, no. 7, pp. 3069-3079, 2019.
- [40] M. Chilali and P. Gahinet, " H_∞ design with pole placement constraints: An LMI approach," *IEEE Transactions on Automatic Control*, vol. 41, no. 3, pp. 358-367, 1996.